

LETTER TO THE EDITOR

A Horseshoe-Shaped Ring of Diffuse Emission Detected at 1.4 GHz

Shobha Kumari¹ and Sabyasachi Pal^{1,*}

Midnapore City College, Kuturia, Bhadutala, Paschim Medinipur, West Bengal, 721129, India *

December 22, 2023

ABSTRACT

We identify a horseshoe-shaped ring (HSR) of diffuse emission in J1407+0453 from the Faint Images of Radio Sky at Twenty-cm (FIRST) survey using the Very Large Array telescope. An optical galaxy SDSSJ140709.01+045302.1 is present near the limb of the HSR of J1407+0453, with a spectroscopic redshift of $z = 0.13360$. The total extent of the source, including the diffuse emission of J1407+0453, is 65 arcsec (with a physical extent of 160 kpc), whereas the diameter of the HSR is approximately 10 arcsec (25 kpc). The flux density of HSR is ~ 47 mJy at 1400 MHz whereas the flux densities of whole diffuse emission of J1407+0453 at 1400 MHz and 150 MHz are 172 mJy and 763 mJy, respectively. We measure the radio luminosity of HSR J1407+0453 as 1.94×10^{24} W Hz⁻¹ with a spectral index $\alpha_{150}^{1400} = -0.67$. The black hole mass of J1407+0453 is $5.8 \times 10^8 M_{\odot}$. We compare the HSR of diffuse emission of J1407+0453 with other discovered diffused circular sources. The possible formation scenarios for J1407+0453 are discussed to understand the nature of the source. We present a spectral index map of source J147+0453 to study the spectral properties of the source.

Key words. galaxies: ISM–galaxies: active–galaxies: clusters: intracluster medium–galaxies: kinematics and dynamics

1. Introduction

Diffuse radio emissions are typically found in radio halos, radio relics, and mini-halos (Feretti & Giovannini 1996; Kempner et al. 2004), depending on their location in the cluster and the type of cluster (merging or cool-core). Clusters that show signs of merging processes are known to have radio halos at their centres (Feretti 2002; Giovannini & Feretti 2002) with an arcmin or more in diameter (Feretti et al. 2021). Relics are located close to the edges of both the merging and relaxed clusters. Mini-halos are centrally placed, hosted in relaxed cool-core clusters, and typically found around powerful radio galaxies. Mini halos are diffuse radio emissions that are typically a few 100 kpc in size. Diffuse extended emissions in the Phoenix cluster (van Weeren et al. 2014), Perseus cluster (Sijbring 1993), RXCJ1720.1+2638 (Giacintucci et al. 2014), and very recently, the Abell 1413 cluster (Riseley et al. 2023), are examples of prototypes of the class of mini-halos. More commonly, the morphology of these diffuse sources has an irregular shape, but some radio relics also have more symmetric and roundish morphologies (e.g. A1664, A2443, Govoni et al. 2001; Cohen & Clarke 2011). Here, it is worth noting that non-thermal diffuse emission can also be present outside the clusters, implying the existence of magnetic fields and relativistic particles in extremely low-density environments.

Apart from the diffuse emission associated with galaxy clusters, some roundish or horseshoe-shaped diffused structures of about one arcmin or more in diameter have been observed in the simulation study of Dolag et al. (2023). Recently a circular symmetry extended diffused radio emission (J1507+3013) around an elliptical galaxy is identified using the Very Large Array (VLA) Faint Images of Radio Sky at Twenty-cm (FIRST) survey (Kumari & Pal 2023). The emergence of such diffuse emissions, by taking a virial mass of $10^{12} M_{\odot}$ may be favoured by merger-

driven internal shocks, as suggested by Dolag et al. (2023). The gravitationally hierarchical emergence of large-scale structures causes shocks in the intergalactic medium (IGM). Shocks can either re-accelerate prior relativistic electron population produced by former active galactic nuclei (AGN) activity within a cluster or directly accelerate IGM thermal electrons (Pizzo et al. 2008). The discovery of radio emissions from intergalactic shocks will have a significant impact on our understanding of cosmology and astrophysics because it will test theories about how structures form, confirm the existence of the previously unknown warm-hot intergalactic medium, and map its distribution (Keshet et al. 2004; Pizzo et al. 2008).

Recently, very faint, edge-brightened diffuse radio emissions, popularly known as odd radio circles (ORCs), have been identified (Norris et al. 2021a,b,c, 2022) using the pilot survey of the Evolutionary Map of the Universe (EMU; Norris et al. 2011). Using this survey, 3 ORCs (ORC1 = ORC J2103–6200, ORC J2058–5736 = ORC2, and ORC J2059–5736 = ORC3) are discovered at high galactic latitudes. Furthermore, MeerKAT observations revealed an inner ring in ORC1. Using Giant Metrewave Radio Telescope (GMRT) archival data at 325 MHz (Norris et al. 2021b,c), Australian Square Kilometre Array Pathfinder (ASKAP) data at 944 MHz (Koribalski et al. 2021), and LO-FAR Two-metre Sky Survey DR2 (LoTSS DR2) at 144 MHz (Omar 2022c), 3 more ORCs are discovered. Earlier, Norris et al. (2021a,b,c, 2022); Omar (2022a,b,c) discussed various scenarios for the formation of ORCs, including the spherical shock wave from the optical host galaxy, termination shock from the starburst wind, and interactions between the optical galaxies inside the ring of the structure (Norris et al. 2021a,b,c, 2022; Koribalski et al. 2021).

The current paper discusses a newly identified horseshoe-shaped ring (HSR) of diffuse emission. The source identification is described in Sect. 2. In Sect. 3, we present our results. In Sect. 4, we compare our results with previously known similar sources

* E-mail: sabya.pal@gmail.com (SP)

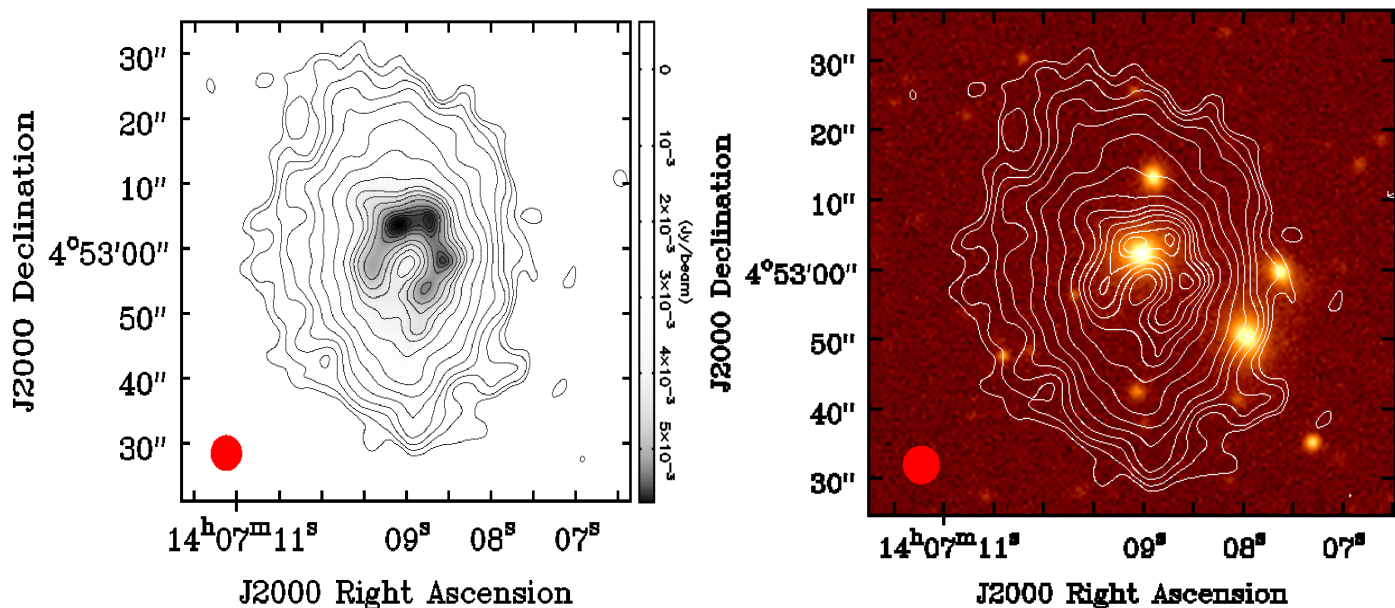


Fig. 1. Left: J1407+0453 at 1400 MHz. The grey scale represents the flux density of the source. Right: J1407+0453 at 1400 MHz in contour overlaid with the optical image taken from the 9th data release of the Dark Energy Spectroscopic Instrument’s Legacy Imaging Surveys (DESI LS DR9; Schlegel et al. 2021). For the both images, the contour levels are at $3\sigma \times (1, 1.4, 2, 2.8, 4, 5.7, 8, 11, 13, 14, 15, 16, 17, 17.5, 18)$, where $\sigma = 133 \mu\text{Jy beam}^{-1}$ is the mean rms noise around the FIRST map.

and discuss the possible formation scenarios of J1407+0453. Section 5 summarises the results of this study. We used the following Λ CDM cosmology parameters for the current paper using the final full-mission Planck measurements of the CMB anisotropies (Aghanim et al. 2020): $H_0 = 67.4 \text{ km s}^{-1} \text{ Mpc}^{-1}$, $\Omega_{vac} = 0.685$, and $\Omega_m = 0.315$.

2. A horseshoe-shaped ring of diffuse emission

We report a newly discovered horseshoe-shaped ring (HSR) of diffuse emission in J1407+0453 from the Faint Images of Radio Sky at Twenty-cm (FIRST) survey at 1.4 GHz using Very Large Array (VLA) radio telescope (Becker et al. 1995; White et al. 1997). An optical galaxy is present near the limb of the horseshoe-shaped inner ring structure of J1407+0453 which may be the host of the diffuse source. The optical galaxy of HSR J1407+0453 has a spectroscopic redshift of 0.13360, obtained from SDSS (Ahumada et al. 2020). The total angular diameter of J1407+0453 is 65 arcsec, with a physical extent of approximately ~ 160 kpc whereas the HSR has an angular diameter of 10 arcsec with a physical extent of ~ 25 kpc. The source diameter is measured by fitting a circle onto the source. Figure 1 shows the FIRST image of the HSR J1407+0453 at 1400 MHz.

The source presented in the current paper (J1407+0453) is also detected in other surveys, such as the Tata Institute of Fundamental Research (TIFR) Giant Metre-wave Radio Telescope (GMRT) Sky Survey (TGSS) at 150 MHz (Intema et al. 2017), the National Radio Astronomy Observatory (NRAO) VLA Sky Survey (NVSS) at 1400 MHz (Condon et al. 1998), the VLA Sky Survey (VLASS) at 3 GHz (Lacy et al. 2020), the Galactic and Extragalactic All-sky Murchison Widefield Array (GLEAM) at 72–231 MHz (Hurley-Walker 2017), and The Rapid ASKAP Continuum Survey (RACS) at 888 MHz (McConnell et al. 2020). All these surveys detected J1407+0453 as a point source, except for VLASS, which shows the diffuse emission structure of the source.

3. Results

3.1. Radio Properties of J1407+0453

We measure the spectral index of the J1407+0453 between 1400 MHz and 150 MHz, using $F_\nu \propto \nu^\alpha$, where F_ν is the integrated flux density at frequency ν and α is the spectral index. The spectral index for total diffuse emission of J1407+0453 is calculated as $\alpha_{150}^{1400} = -0.67 \pm 0.05$ using integrated radio flux densities of 172 and 763 mJy at 1400 MHz and 150 MHz, respectively, of the total diffuse emission of J1407+0453. Here, we use NVSS (Condon et al. 1998) flux density instead of FIRST because the FIRST survey is prone to flux density loss owing to the lack of short spacing (short baselines). The radio luminosity of the total diffuse emission of J1407+0453 at 1400 MHz is measured as $7.09 \times 10^{24} \text{ W Hz}^{-1}$ with the help of standard formula (Donoso et al. 2009);

$$L_{\text{rad}} = 4\pi D_L^2 F_\nu (1+z)^{\alpha-1} \quad (1)$$

where F_ν is the flux density ($\text{W m}^{-2} \text{ Hz}^{-1}$) at a given frequency, D_L is the luminosity distance to the source in metres (m), α is the spectral index, and z is the redshift of J1407+0453 ($z = 0.13360$). The flux density of the HSR of J1407+0453 at 1400 MHz is measured as ~ 47 mJy. Using the flux density of the HSR, we calculate the radio luminosity of the HSR of J1407+0453 to be $1.94 \times 10^{24} \text{ W Hz}^{-1}$.

3.2. Spectral index map of J1407+0453

We present the spectral index map of J1407+0453 in Fig. 2 between 1400 MHz and 150 MHz. The typical error in the spectral index map is ~ 0.02 . The error is nearly uniform, except at the edge of the radio emission, where it reaches 0.08. The contour plot in Fig. 2 shows the VLA FIRST image of J1407+0453 at 1400 MHz. The spectral index of HSR is ranging from -0.4 to -0.5 . The spectral index inside the ring is -0.65 , whereas the spectral index of the outer region of the HSR becomes steeper

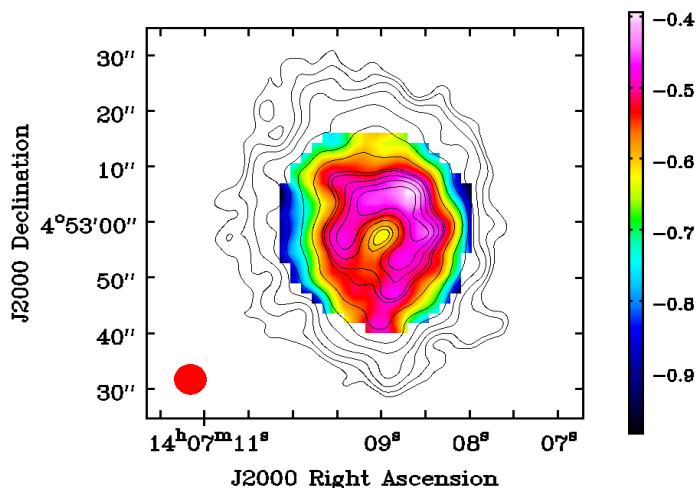


Fig. 2. Spectral index map of J1407+0453 overlaid with the FIRST image in contour. The lowest contour level in the figure is at 3σ , where σ is the rms noise of the source in the FIRST map. The rms noise of the source in the VLA FIRST image is $133 \mu\text{Jy beam}^{-1}$. The contour levels are at $3\sigma \times (1, 1.4, 2, 2.8, 4, 5.7, 8, 11, 13, 14, 15, 16, 17, 17.5, 18)$. The colour scale represents the spectral index of J1407+0453.

ranging from -0.55 to -0.95 . Spectral steepening from the core towards the edge of the lobes is observed in radio galaxies, which is thought to be due to spectral ageing in the structure of the source. The steepening in the outer region of the HSR is also possibly due to spectral ageing in the structure of the source.

3.3. Optical Properties of J1407+0453

We identify the optical counterpart of J1407+0453 from the Dark Energy Camera Legacy Survey (DECaLS) (Dey et al. 2019). An overlaid image of J1407+0453 at 1.4 GHz with DECaLS is shown in the right panel of Fig. 1. The optical galaxy SDSS J140709.01+045302.1 resides near the geometrical centre of J1407+0453 (labelled as ‘core’ in Fig. 3), with a spectroscopic redshift of 0.13360. The location of SDSS J140709.01+045302.1 also coincides with the radio core of J1407+0453. Within one arc minute distance from the optical galaxy SDSSJ140709.01+045302.1, there are 6 optical/IR sources labelled as ‘A’, ‘B’, ‘C’, ‘D’, ‘E’ and ‘F’ (see Fig. 3). The bright optical/infrared source labelled as ‘A’ (2MASS 140708.914+045313.48) is at 11 arcsec angular distance (31 kpc projected distance) far from the optical galaxy SDSS J140709.01+045302.1. The photometric redshift of the optical galaxy ‘A’ is 0.158 ± 0.021 . A galaxy labelled as ‘B’ (see Fig. 3) is located towards the south-east of ‘A’ and 20.86 arcsec (54 kpc projected distance) angular distance far from the optical galaxy SDSSJ140709.01+045302.1. This galaxy is 2MASS J14070763+0452592, with a photometric redshift of 0.141 ± 0.012 . An optical galaxy labelled as ‘C’ (see Fig. 3) is located towards the south-west of ‘B’ and 19 arcsec angular distance (44 kpc projected distance) far from the optical galaxy SDSSJ140709.01+045302.1. This galaxy is WISEA J140707.95+045250.5, or 2MASS J14070795+0452505, with a photometric redshift of 0.125 ± 0.008 . Three more galaxies labelled as ‘D’, ‘E’ and ‘F’ (see Fig. 3) are located at 19.92 arcsec (78.3 kpc projected distance), 25.54 arc-

sec (51.51 kpc projected distance) and 23.62 arcsec (116.5 kpc projected distance) apart from the optical galaxy SDSS J140709.01+045302.1. The photometric redshifts of galaxies ‘D’, ‘E’ and ‘F’ are 0.240 ± 0.071 , 0.106 ± 0.118 , and 0.331 ± 0.190 , respectively. The optical galaxy ‘D’ is 2MASS J140709098+045242.27, ‘E’ is 2MASS J140710446+045248, and ‘F’ is WISEA J140709.10+045325.3. Photometric redshifts are taken from the Dark Energy Camera Legacy Survey data released 9 (DECaLS DR9; Dey et al. (2019)) and spectroscopic redshift of SDSS J140709.01+045302.1 (labelled as ‘core’ in Fig. 1) is taken from SDSS (Ahumada et al. 2020).

We measure the approximate black hole mass for the optical host galaxy (SDSSJ140709.01+045302.1) of J1407+0453 using the $M_{BH}-\sigma_*$ relation (Gebhardt et al. 2000; Ferrarese & Merritt 2000),

$$\frac{M_{BH}}{10^8 M_\odot} = 3.1 \left(\frac{\sigma_*}{200 \text{ km s}^{-1}} \right)^4 \quad (2)$$

where σ_* is the velocity dispersion, and M_\odot is the stellar mass ($\sim 2 \times 10^{31}$ kg). We use the stellar velocity dispersion (σ_*) information from the SDSS (Ahumada et al. 2020) to compute M_{BH} . The black-hole mass of J1407+0453 is measured as $5.8 \times 10^8 M_\odot$ ($\sim 10^{8.8} M_\odot$) with a stellar velocity dispersion (σ_*) of 233.46 ± 8.70 km/s.

3.4. Mid-IR Properties of J1407+0453

To study the host properties of J1407+0453 at mid-IR wavelengths, we use the Wide-field Infrared Survey Explorer (WISE; Wright et al. 2010), which is an all-sky infrared survey. WISE is a space-based telescope which can observe in four bands (W1, W2, W3, and W4) that correspond to $3.4 \mu\text{m}$, $4.6 \mu\text{m}$, $12 \mu\text{m}$, and $22 \mu\text{m}$ wavelengths, respectively. We measured mid-IR colours $W1-W2 = 0.13$, and $W2-W3 = 1.24$, which suggests that J1407+0453 may be a low-excitation radio galaxy (LERG) (Prescott et al. 2018; Dabhade et al. 2020). It should be noted that WISE data alone are not sufficient to classify the host galaxy of J1407+0453; we need a detailed optical study to understand the nature of the host galaxy of J1407+0453.

4. Discussions

4.1. HSR J1407+0453 versus previously discovered diffused sources

Nearly circular-shaped diffuse emission (for example, Fig 8a and 8b of Sadler et al. (2002)) is not uncommon, but a ring-like structure within a circular-shaped diffuse emission is rare. Recently, large circular patches of radio emission, popularly known as odd radio circles (ORCs), have been detected (Norris et al. 2011). They appear as ring-like structures with a bright edge; along with an interior that is either faint or empty of radio emission. Among the 6 previously discovered ORCs, 3 are associated with optical galaxies near their geometrical core, and the diffused source, J1407+0453 in the current study is also associated with an optical galaxy near the core. Here, we compare the morphological features and properties of J1407+0453 with those of 3 previously discovered optically hosted ORCs (ORC J2103–6200 (ORC1), ORC J1555+2726 (ORC4), and ORC J0102–2450 (ORC5)).

The inner edge of J1407+0453 is bent with 3 bright compact radio counterparts, making it a horseshoe-shaped ring (see left and right panel of Fig. 1), whereas the outer edge of the ring of ORC5 is bent (like a wide-angle tailed (WAT)). The similarity

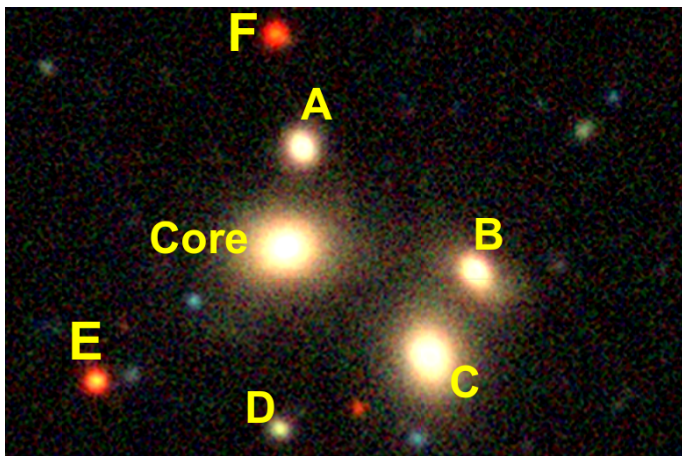


Fig. 3. Optical image of J1407+0453 region taken from DESI LS DR9 (Schlegel et al. 2021).

between J1407+0453 and ORCs 1, 4, and 5 is that all sources have a radio core inside the ring, but the possible optical galaxy resides at the limb of the HSR in J1407+0453 and not on the radio core (see right panel of Fig. 1), whereas, in ORCs 1, 4, and 5, the optical counterpart coincides with the radio core. Initially, only one outer ring was observed in ORC1, but in the MeerKAT observation, apart from the outer ring, an arc-like structure inside the ring (also referred to as a polar ring) was observed, whereas J1407+0453 contains only the horseshoe-shaped inner ring without an outer ring.

The WISE colours for J1407+0453 ($W1-W2 = 0.13$, $W2-W3 = 1.24$) and ORC1 ($W1-W2 = 0.081$, $W2-W3 < 2.045$) for the central object suggest that both of the sources are low-excitation radio galaxy (LERG) ($W1-W2 < 0.5$ and $0.2 < W2-W3 < 4.5$) (Prescott et al. 2018; Dabhade et al. 2020). The HSR of diffuse emission of J1407+0453 has a flux density of ~ 47 mJy at 1400 MHz FIRST image, whereas the total diffusion emission of J1407+0453 has radio flux densities of 172 mJy and 763 mJy at 1400 MHz and 150 MHz, respectively. Therefore, J1407+0453 has a significantly higher flux density than ORC1, ORC4, and ORC5, which have flux densities in the range of 1.9 mJy to 7 mJy at ~ 1 GHz. The spectral index of HSR of diffuse emission of J1407+0453 ranges from -0.4 to -0.5 whereas the outer region of the HSR has a spectral index in the range of -0.55 to -0.95 . So, J1407+0453 has a flatter radio spectrum in the periphery of the HSR and along the outer region of the HSR compared to the spectral indices of ORC1, ORC4, and ORC5, as they have very steep spectral index ≤ -0.9 (Norris et al. 2021a,b,c, 2022; Koribalski et al. 2021).

The physical extent of the HSR ring of J1407+0453 is ~ 25 kpc with a spectroscopic redshift of 0.13360, whereas the physical extents of ORC1, ORC4, and ORC5 lie in the range of 100–450 kpc (with available photometric redshifts in the range of 0.39–0.55).

The black-hole mass of J1407+0453 is $5.8 \times 10^8 M_{\odot}$ whereas that of ORC5 is $7.5 \times 10^8 M_{\odot}$. The radio luminosity of the HSR of J1407+0453 is $1.94 \times 10^{24} \text{ W Hz}^{-1}$ and that of the total diffuse emission of J1407+0453 is $7.09 \times 10^{24} \text{ W Hz}^{-1}$ whereas for ORC1, ORC4, and ORC5, the radio luminosity $\sim 10^{23} \text{ W Hz}^{-1}$. Thus, the black hole in J1407+0453 is less massive, but the ring is more luminous than those of ORC1, ORC4, and ORC5.

Morphologically, J1407+0453 and the previously discovered ORCs have similarities with a ring of diffuse emission. However, as we compare J1407+0453 with ORC1, ORC4, and

ORC5 above, J1407+0453 is more luminous, with a significantly strong flux density and a less steep spectrum. J1407+0453 also exhibits a horseshoe-shaped inner ring of about ~ 25 kpc in size (much smaller than the ring observed in previously discovered ORCs; 100–450 kpc), and none of the ORCs exhibit such a horseshoe-shaped inner ring. Although the horseshoe-shaped ring of J1407+0453 is much smaller than that of ORCs, the size of the total diffuse emission of J1407+0453 is ~ 160 kpc, which is comparable in size to ORCs. However, we should be careful about the fact that there are only 3 ORCs known so far that are hosted by the optical galaxies, and among them, only one source (ORC4) possesses a radio core that coincides with the optical galaxy. More sources with similar properties are required to understand the nature of ORCs along with J1407+0453. It is also possible that J1407+0453 may be in its early phase, yet to lose its energy and become a low-power faint ORC, similar to other discovered ORCs.

Diffuse radio emissions have also been observed in galaxy clusters such as mini-haloes (Kempner et al. 2004). Mini-haloes are often seen around radio galaxies within clusters. It should be noted that these mini haloes are significantly larger (≥ 100 kpc in size) (Riseley et al. 2023) than J1407+0453. It is also difficult to classify J1407+0453 as a mini halo because J1407+0453 is not associated with any galaxy cluster.

Another possibility is that the diffuse emission of J1407+0453 may represent the remains of a "fossil" radio galaxy (Kempner et al. 2004; Riseley et al. 2023), but that would be expected to have a very steep spectral index (< -1.5), which is not supported by the results presented in the current paper for J1407+0453.

4.2. Formation Scenarios of J1407+0453

In the following, we discuss some plausible formation scenarios for J1407+0453. One of the possibilities for the formation of J1407+0453 can be the shocks produced in post-starburst galaxies by tidal disruption events around the core of the supermassive black holes (as previously discussed for the formation of circular diffused sources like ORCs) (Omar 2022a,b). This can also be considered for diffuse sources with optical host galaxies near their geometrical centre, as observed in J1407+0453.

Another possible hypothesis is that J1407+0453 can be the result of a giant blast wave in the central galaxy (Norris et al. 2021a,b,c, 2022; Koribalski et al. 2021). Consequently, it produces a horseshoe-shaped ring (HSR) of diffuse radio emission which appears as edge-brightened discs similar to planetary nebulae or SNRs. This radio emission is likely produced due to the synchrotron emission caused by the accelerated electrons by the shock (Downes et al. 2002; Cao & Wang 2012; Ricci et al. 2021). A binary SMBH merger in the centre of the galaxy can produce such a spherical shock (Bode et al. 2012); thus, we would expect to observe a magnetic field in the ring that is largely tangential and orthogonal to the velocity of the shock, such as SNRs or cluster relics.

Recently, a simulation study of Dolag et al. (2023) explained the internal merger shocks produced around some galaxies by matching several observed properties of the neighbouring galaxy. This simulation study shows that shocks produced by strong galactic merger events cause circular radio emission (structure) with a virial mass of $10^{13} M_{\odot}$ (Dolag et al. 2023). In their simulation, a major merger event at $z = 0.7$ is possibly responsible for driving two subsequent shocks far beyond the virial radius propagation (Dolag et al. 2023). In this propagation, about arcmin-sized roundish- or horseshoe-shaped struc-

tures of diffuse emission are produced (Dolag et al. 2023), similar to J1407+0453 presented in the current paper. Noteworthy, Dolag et al. (2023) discovered radio rings that are far fainter and larger than the horseshoe-shaped ring observed in J1407+0453.

There are 6 nearby optical sources within an angular diameter of 1 arcmin from the optical core of J1407+0453 (as discussed in Sect. 3.3). The nearest optical galaxies are ‘A’ (photometric redshift of 0.158 ± 0.021) and ‘C’ (photometric redshift of 0.125 ± 0.008) with projected distances of 31 and 44 kpc, respectively, from the optical host galaxy. The presented uncertainties on the redshifts for optical galaxies ‘A’, ‘B’, ‘C’, ‘D’, ‘E’ and ‘F’ (see Fig. 3) suggest that these galaxies are several Mpc from each other. However, uncertainties are often underestimated, and thus, galaxies may be associated. Therefore, it is possible that J1407+0453 is the result of the production of shock waves that lead to the ring-like diffuse structure of J1407+0453, as discussed above and observed in Dolag et al. (2023).

Here, it should be noted that the elliptical host galaxy of J1407+0453 is located on the limb of the horseshoe shape rather than being in the centre. Therefore, this morphology may not be consistent with the emission of a spherical shockwave from an elliptical optical galaxy.

The horseshoe-shaped inner ring of J1407+0453 resembles the morphology of narrow angle-tailed (NAT) sources (Missaglia et al. 2019; Bhukta et al. 2022; Sasmal et al. 2022; Pal & Kumari 2023). However, most of the previously discovered NAT sources are associated with a cluster of galaxies, and for J1407+0453 no associated galaxy cluster is identified. For NAT sources, the optical counterparts are located near the centre of the bent structure between the two warm spots (Bhukta et al. 2022). However, the horseshoe-shaped ring of J1407+0453 does not contain any symmetrical warm spots and the optical counterpart in J1407+0453 is offset from the centre. The optical counterpart is neither inside the ring nor located on the periphery of the ring, instead, the optical counterpart is located on the limb of the horseshoe-shaped ring. Therefore, J1407+0453 may not be a head-tailed source.

As J1407+0453 is unlikely to fall in the above-discussed classes of diffuse sources, it may represent a new class of strong and luminous extended diffuse sources hosted by an optical galaxy near the centre of the structure.

5. Conclusions

A diffuse source, J1407+0453 with a horseshoe-shaped inner ring is reported in this paper from the VLA FIRST survey at 1.4 GHz. The total angular diameter of J1407+0453 is 65 arcsec, whereas that of the horseshoe-shaped ring is ~ 10 arcsec (which is smaller than that of the previously known ring of ORCs). J1407+0453 is associated with an optically dense region with a bright compact optical host galaxy identified near the limb of the horseshoe-shaped ring and 6 nearby optical galaxies within an angular distance of 1 arcmin from the core of the optical host galaxy. J1407+0453 can be the early/young phase of an ORC object hosted by an optical galaxy or it can be a new class of object that needs to be studied in detail with more samples. The structure of such diffuse emission, as presented in the current paper in J1407+0453, can also be seen in the class of mini halos and fossil radio galaxies. J1407+0453 may not be a mini halo or fossil radio galaxy because J1407+0453 is not associated with any galaxy cluster (required for mini halos sources), and J1407+0453 does not possess a steep spectrum (< -1.5) (needed for fossil radio galaxies). In this paper, we discuss some possible scenarios for the formation of J1407+0453.

Further follow-up multi-wavelength observations are encouraged to study the nature of the diffuse emission of J1407+0453. Deep X-ray observations and studies are also required to detect any energetic events inside the horseshoe-shaped ring of J1407+0453 that may cause the diffuse emission in the structure.

Acknowledgements. We thank the anonymous reviewer for helpful suggestions. This paper used Sloan Digital Sky Survey V data. Funding for the Sloan Digital Sky Survey V has been provided by the Alfred P. Sloan Foundation, the Heising-Simons Foundation, the National Science Foundation, and the Participating Institutions. SDSS acknowledges support and resources from the Center for High-Performance Computing at the University of Utah. The photometric redshifts for the Legacy Surveys (PRLS) catalogue are used in this paper. The PRLS is funded by the U.S. Department of Energy Office of Science, Office of High Energy Physics via grant DE-SC0007914.

References

- Aghanim, N., Akrami, Y., Ashdown, M., et al. 2020, *A&A*, 641, 67
 Ahumada, R., Allende, P. C., Almeida, A., et al. 2020, *ApJS*, 249, 21
 Bode, T., Bogdanović, T., Haas, R., et al. 2012, *ApJ*, 744, 45
 Becker, R. H., White, R. L., & Helfand, D. J., 1995, *ApJ*, 450, 559
 Bhukta, N., Pal, S., Mondal, S., 2022, *MNRAS*, 516, 372
 Cao, D., & Wang, X. Y., 2012, *ApJ*, 761, 111
 Cohen, A. S., & Clarke, T. E., 2011, *AJ*, 141, 149
 Condon, J. J., Cotton, W. D., Greisen, E. W., et al. 1998, *AJ*, 115, 1693
 Dabhade, P., Mahato, M., Bagchi, J., et al. 2020, *A&A*, 635, A5
 Dey, A., Schlegel, D. J., Lang, D., et al. 2019, *AJ*, 157, 29pp
 Dolag, K., Boss, L. M., Koribalski, B. S., Steinwandel, U. P., Valentini, M., 2023, *ApJ*, 945, 74
 Downes, T. P., Duffy, P., & Komissarov, S. S., 2002, *MNRAS*, 332, 144
 Donoso, E., Best, P. N., & Kauffmann, G., 2009, *MNRAS*, 392, 617
 Ferrarese, L., & Merritt, D. 2000, *ApJ*, 539, L9
 Feretti, L., & Giovannini, G. 1996, in *Extragalactic Radio Sources*, ed. R. D. Ekers, C. Fanti, & L. Padrielli, IAU Symp., 175, 333
 Feretti, L., 2002, In: *Universe Low Radio Freq.* IAU, 199, 133
 Feretti, L., Giovannini, G., Govoni, F., & Murgia, M. 2012, *A&ARv*, 20, 54
 Gebhardt, K., Bender, R., Bower, G., et al. 2000, *ApJ*, 539, L13
 Giacintucci, S., Markevitch, M., Brunetti, G., et al. 2014, *ApJ*, 795, 73
 Giovannini, G., & Feretti, L., 2002, In: *Astrophys space sci libr*, vol 272. Kluwer Academic, Dordrecht, p 197
 Govoni, F., Feretti, L., Giovannini, G., et al. 2001, *A&A*, 376, 803
 Hurley-Walker N., 2017, *MNRAS*, 464, 1146
 Intema, H. T., Jagannathan, P., Mooley, K. P., Frail, D. A. 2017, *A&A*, 598, A78
 Kempner, J. C., Blanton, E. L., Clarke, T. E., Enßlin, T. A., Johnston-Hollitt, M., Rudnick, L., 2004, in Reiprich, T., Kempner, J., Soker, N., eds, *The Riddle of Cooling Flows in Galaxies and Clusters of galaxies*. p. 335
 Keshet, U., Waxman, E., & Loeb, A. 2004, *New Astron. Rev.*, 48, 1119
 Koribalski, B. S., Norris, R. P., Andernach, H., et al. 2021, *MNRAS*, 505, L11
 Kumari, S., & Pal, S., 2023, *MNRAS*, submitted
 Lacy, M., Baum, S. A., Chandler, C. J., et al. 2020, *PASP*, 132, 035001
 McConnell, D., Hale, C., Lenc, E. et al. 2020, *PASA*, 37, E048
 Missaglia, V., Massaro, F., Capetti, A., et al. 2019, *A&A*, 626, A8
 Norris, R. P., Hopkins, A. M., Afonso, J., et al. 2011, *PASA*, 28, 215
 Norris, R. P., Marvil, J., Collier, J. D., et al. 2021a, *PASA*, 38, e046
 Norris, R. P., Intema, H. T., Kapińska, A. D., et al., 2021b, *PASA*, 38, E003
 Norris, R. P., Crawford, E., & Macgregor, P. 2021c, *Galaxies*, 9, 83
 Norris, R. P., Collier, J. D., Crocker, R. M., et al., 2022 *MNRAS*, 513, 1300
 Omar, A., 2022a, *MNRAS*, 513, L101
 Omar, A. 2022b, *MNRAS*, 516, L43
 Omar, A. 2022c, *RNAAS*, 6, 100
 Pal, S., Kumari, S., 2023, *JoAA*, 44, 17
 Pizzo, R. F., de Bruyn, A. G., Feretti, L., & Govoni, F. 2008, *A&A*, 481, L91
 Prescott, M., Whittam, I.H., Jarvis, M.J., McAlpine, K., Richter, L.L., Fine, S., Mauch, T., Heywood, I., Vaccari, M., 2018, *MNRAS*, 480, 707
 Ricci, R., Troja, E., Bruni, G., et al., 2021, *MNRAS*, 500, 1708
 Riseley, C. J., Biava, N., Lusetti, G., et al. 2023, *MNRAS*, 524, 6052
 Sadler E. M., Jackson, C. A., Cannon, R.D., et al. 2002 *MNRAS* 329, 227
 Sasmal, T. K., Bera, S., Pal, S., Mondal, S., 2022, *ApJS*, 259, 31
 Schlegel, D., Dey, A., Herrera, D., et al. 2021, in *American Astronomical Society Meeting Abstracts*, Vol. 53, American Astronomical Society Meeting Abstracts, 235.03
 Sijbring, L. G., 1993, A radio continuum and HI line study of the perseus cluster. PhD thesis, Groningen: Rijksuniversiteit.
 van Weeren, R. J., Intema, H. T., Lal, D. V., et al. 2014, *APJL*, 786, L17
 White, R. L., Becker, R. H., Helfand, D. J., Gregg, M. D., 1997, *ApJ*, 475, 479
 Wright, E. L., Eisenhardt, P. R. M., Mainzer, A. K., et al. 2010, *AJ*, 140, 1868